The expression of *RUNDC3B* is associated with promoter methylation in lymphoid malignancies

Running Head: Epigenetic regulation of *RUNDC3B*

Keywords: RUNDC3B, DNA methylation, lymphoma, leukemia, B-cell, gene expression

Dane W. Burmeister[1], Emily H. Smith[1,2], Robert T. Cristel[1], Stephanie D. McKay[1,3], Huidong Shi[4], Gerald L. Arthur[1], J. Wade Davis[5,6], and Kristen H. Taylor[1,*]

[1]Department of Pathology and Anatomical Sciences; University of Missouri; Columbia, MO USA; [2]Department of Dermatology; University of Michigan Health System; Ann Arbor, MI USA; [3]Department of Animal Science; University of Vermont; Burlington, VT USA; [4]Department of Biochemistry and Molecular Biology; Georgia Regents University; Augusta, GA USA; [5]Department of Health Management and Informatics; University of Missouri; Columbia, MO USA; [6]Department of Statistics; University of Missouri, Columbia, MO USA

***Corresponding author:**
Kristen H. Taylor PhD
Department of Pathology and Anatomical Sciences
One Hospital Drive
University of Missouri-Columbia
Columbia, Missouri 65212 USA
E-mail: taylorkh@health.missouri.edu
Telephone: 573-882-5523
FAX: 573-884-4612

This work was supported by a National Institute of Health grant NCI R00 CA132784 (K.H. Taylor)

No potential conflicts exist for the authors of this manuscript.

Word Count: 2991

Abstract

DNA methylation is an epigenetic modification that plays an important role in regulation of gene expression. The function of *RUNDC3B* has yet to be determined, although its dysregulated expression has been associated with malignant potential of both breast and lung carcinoma. To elucidate the potential of using DNA methylation in *RUNDC3B* as a biomarker in lymphoid malignancies, the methylation status of six regions spanning the CpG island (CGI) in the promoter region of *RUNDC3B* was determined in cancer cell lines. Lymphoid malignancies were found to have more prominent methylation and did not express *RUNDC3B* compared to myeloid malignancies and solid tumors supporting the potential use of DNA methylation in this region as a biomarker for lymphoid malignancies. RUNDC3B contains a RUN-domain in its N-terminal region that mediates interaction with Rap2, an important component of the MAPK cascade which regulates cellular proliferation and differentiation. The protein sequence of RUNDC3B also contains characteristic binding sites for MAPK intermediates. Therefore, it is possible that RUNDC3B serves as a mediator between Rap2 and the MAPK signaling cascade. Three genes with MAPK inducible expression were downregulated in a methylated leukemia cell line (HSPA5, Jun and Fos). Jun and Fos combine to form the AP-1 transcription factor and loss of this factor is associated with the dysregulation of genes involved in differentiation and proliferation. We hypothesize that the loss of RUNDC3B secondary to aberrant hypermethylation of the EGR-3 transcription factor binding site results in dysregulated MAPK signaling and carcinogenesis in lymphoid malignancies.

Introduction

DNA methylation is an epigenetic modification that can alter chromatin structure and physically block the access of transcriptional machinery. This modification most often occurs on cytosine residues followed by guanine residues (CpG dinucleotides) in mammals. CpG dinucleotides are not evenly distributed throughout the genome, but occur in clusters known as CpG islands (CGI). CGIs present within the promoter region of genes are normally unmethylated and actively transcribed. The disruption of normal methylation patterns is a hallmark of tumorigenesis and the gain of methylation in gene promoters, often leads to the silencing of tumor suppressor genes [1]. These aberrant methylation events can be used as biomarkers and have proven useful in identifying cancer types, risk assessment, diagnosis, and response to drug treatment.

Methylation of *RUNDC3B* has been reported in acute lymphoblastic leukemia (ALL) and is associated with a reduction in gene expression [2]. Interestingly, treatment of ALL cell lines with a demethylating agent restored expression of the *RUNDC3B* gene suggesting that methylation within the promoter of this gene plays a role in the regulation of *RUNDC3B* expression in ALL. Furthermore, methylation of *RUNDC3B* was not observed in acute myeloid leukemia suggesting the putative utility of *RUNDC3B* methylation as a biomarker in lymphoid malignances [3].

RUNDC3B is expressed in many different tissues including brain, thymus, ovary, testis, leukocytes, liver, small intestines, and prostate [4]. It shares high homology with *RUNDC3A*, a

Rap2 interacting protein and is predicted to also interact with Rap2. The Rap protein family constitutes a subgroup of the Ras superfamily which are small GTPases that work as molecular switches to regulate many cellular functions such as proliferation, differentiation, and cell motility [5]. The dysregulation of these cellular functions is commonly associated with cancer formation.

In this study we sought to determine if *RUNDC3B* methylation was unique to lymphoid malignancies and to elucidate the molecular mechanisms that contribute to the silencing of the gene. To accomplish these goals, the methylation status of malignant and normal cell lines and of normal B-cells isolated from healthy individuals was determined and correlated with expression data. The data suggest that *RUNDC3B* methylation may have a role in the pathogenesis of lymphoid malignancies.

Materials and methods

Sample preparation

Cell lines comprised 9 lymphoid malignancies (MHHCall 3, Nalm 6, Jurkat, Mec-1, DB, Granta-519, RL, Raji, Daudi), 2 myeloid malignancies (U266B1, KG-1), 5 solid tumors (MDA-MB 231, Hela, A431, A549, WiDr), and 2 control lymphoid cell lines (GM06990, GM00536). One cord blood and one bone marrow sample were also included (**Table 1**). DNA and RNA extractions were performed with the DNeasy Blood and Tissue Kit and the RNeasy Mini Kit. All samples were collected in accordance with approval from the University of Missouri's Institutional Review Board.

Methylation assays

Bisulfite treatment was performed on 1 µg of DNA using the ZYMO EZ DNA Methylation Gold kit. CT conversion reagent was added to each sample and incubated at 98^{o} C for 10 minutes followed by 64^{o} C for 2.5 hours. Each sample was then desulfonated and eluted in a final volume of 50 µl.

MethPrimer (http://www.urogene.org/methprimer/) was utilized to design combined bisulfite and restriction analysis (COBRA) and methylation specific PCR (MSP) primers (**Table 2**). The 25.0 µl reaction included 2.5 µl of 25.0 mM $MgCl_2$, 2.5 µl of PCR Gold Buffer, 0.5 µl of 10mM dNTPs, 0.75µl of 10 µM forward and reverse primers, 0.125 µl of AmpliTaq Gold, and 3.0µl DNA template. Thermal cycling was performed with a 10 minute hot start at 95^{o} C, followed by 4 touchdown cycles of: 95^{o} C for 15 seconds, 60 ^{o} C (regions 1, 2, and 6) or 64^{o} C (region 5) decreasing one degree each cycle for 30 seconds, and 68 ^{o} C for 30 seconds. This was followed by 32 cycles of: 95^{o} C for 15 seconds, 56 ^{o} C (regions 1, 2, and 5) or 60 ^{o} C (region 4) for 30 seconds, and 68 ^{o} C for 30 seconds. A final extension at 68^{o} C for 7 minutes was included. All PCR amplifications were visualized on a 1.5% agarose gel.

Restriction enzyme digest reactions were performed to determine whether the amplified region contained methylated cytosines. Each amplicon generated for regions 1, 2, 5 and 6 contained a BstUI restriction site, CG*CG. The 25.0µl reaction included 6.0 µl of PCR product, 1.0 µl of Bst-UI enzyme, and 2.5 µl of NEB2 buffer. The reactions were incubated for 4 hours at 60^{o} C and visualized on a 2.5% agarose gel. Samples were categorized as methylated if they

exhibited the expected enzyme digest banding pattern (**Table 2**). If the PCR product was present and no enzyme digest banding pattern was observed the sample was categorized as unmethylated. Finally, samples that exhibited the digested banding pattern and the undigested PCR product were considered partially methylated.

No acceptable COBRA primers were generated for the interval between region 2 and 5; therefore MSP primers were developed for regions 3 and 4. Thermal cycling was performed with a 10 minute hot start at 95^{o} C, followed by 4 touchdown cycles of: 95^{o} C for 15 seconds, 60^{o} C for 30 seconds-decreasing one degree each cycle, and 68 ^{o} C for 30 seconds. This was followed by 32 cycles of: 95^{o} C for 15 seconds, 56^{o} C for 30 seconds, 68 ^{o} C for 30 seconds. A final extension of 68^{o} C for 7 minutes was included. All PCR amplifications were visualized on a 1.5% agarose gel. Samples were categorized as methylated if there was an appropriately sized amplicon produced by the methylated primer pair. Likewise, if the unmethylated primer pair amplified the sample it was categorized as unmethylated. Finally, if amplicons were visible for both primer sets the samples were considered partially methylated.

Expression assays

Quantitative real-time PCR using Taqman primer/probe sets (Applied Bio systems RUNDC3B Hs00379227_m1 and GAPDH Hs0392909_g1) was performed to detect mRNA expression. The 20 µl reactions included 40.0 ng RNA template, 4.0µl of Taqman reaction buffer, 2.4 µl of magnesium acetate, 0.6 µl of each 10 mM dNTP, 0.8 µl of rth polymerase and 0.2 µl Uracil-N-Glycosylase (UNG). All reactions were conducted on the iCycler iQ and

processed by iCycler software v 3.1. Thermal cycling began with 50°C for 2 minutes to activate UNG; 60°C for 30 minutes to perform the reverse transcription; and 95°C for 5 minutes to deactivate UNG. This was followed by 40 cycles of: 20 seconds at 94°C for 20 seconds and 62°C for 1 minute. All reactions were performed in triplicate. Cycle thresholds (C_T) were established for each gene in each sample. If the C_T value was N/A or greater than 35, the value was recorded as 35. The ΔCt value was calculated for each sample by subtracting the C_T from *GAPDH* from the C_T for *RUNDC3B.*

Statistical methods

The methylation status for each sample was recorded in the six PCR regions as unmethylated, partially methylated, or methylated. An ad hoc methylation density score was attributed to each sample to describe the methylation across the CGI. Each region was given a numerical value (1= methylated, 0.5=partially methylated, and 0=unmethylated) and the methylation density was calculated by averaging the numerical values across all regions for each sample.

Odds ratios were calculated based on dichotomous criteria for PCR region methylation and *RUNDC3B* expression status. The methylation data was categorized as either a methylated region (which also included partially methylated) or unmethylated region. The expression data was defined as *RUNDC3B* expressing (Ct < 35) and *RUNDC3B* non-expressing (Ct > 35). The odds ratios including 95% confidence intervals and p-values were calculated using MedCalc software v 12.4. In instances with zero observations for any cell in the contingency table, a

constant equal to 0.5 was added to each cell [6]. Spearman's rank correlation was performed using SPSS software. Fisher's exact test and exact Mann-Whitney were computed in R 3.0.1 using the `coin` package.

MAPK signaling pathway PCR array

The relative expression of 84 genes related to the MAPK pathway was determined by comparing expression levels in the methylated Nalm 6 cell line versus unmethylated healthy bone marrow using RT^2 Profiler PCR Arrays. RNA was converted to cDNA using the Superscript III First-Strand Synthesis System following the protocol provided. The cDNA was added to the qPCR master mix provided with MAPK PCR array and aliquoted into the plate containing optimized RT primers for genes involved in the MAPK pathway and housekeeping genes. The plates were run on a Bio Rad iCycler iQ with a 10 minute hot start at 95^{o}C followed by 40 cycles of 95^{o}C for 15 seconds and 60 ^{o}C for 1 minute. The data was analyzed using the $\Delta\Delta C_T$ method.

Results

Methylation of *RUNDC3B* is prevalent in lymphoid malignancies

In our previous work we showed that *RUNDC3B* promoter methylation is present in lymphoid cell lines and ALL patient samples but not in myeloid cell lines [2,3]. To ascertain the extent of methylation across the *RUNDC3B* (NM_138290.2) promoter and to determine if methylation is unique to lymphoid malignancies, primers were developed to encompass the CGI that spans the transcriptional start site (**Figure 1)**. This region was assayed for methylation using

COBRA (Regions 1, 2, 5, 6) and MSP (Regions 3, 4). Higher levels of methylation were observed in the lymphoid malignancies than in the myeloid malignancies and normal controls consistent with our previous findings (**Figure 2**). Methylation was also observed in some solid tumors with the greatest amount in lung, colon and squamous cell carcinoma. The overall density of methylation was higher in lymphoid malignancies averaging 0.69 across the 6 regions analyzed while solid tumors, myeloid malignancies and healthy tissues had average methylation densities of 0.22, 0.08 and 0.0 respectively. Using an exact Mann-Whitney test on the methylation density average score, higher levels of methylation were observed in the lymphoid malignancies than in the solid tumors ($p=.029$), normal controls ($p=4.99x10^{-4}$) and myeloid malignancies ($p=.109$).

Methylation density impacts *RUNDC3B* expression

Real-time PCR was performed to determine the effect of methylation on *RUNDC3B* expression. In the lymphoid malignancies, no expression was observed in cell lines with a high methylation density score (**Figure 2**). With the exception of A431 all solid tumor cell lines expressed *RUNDC3B* regardless of methylation density. Expression data for *RUNDC3B* (ΔCt values) were ranked and correlated to ranked methylation density scores using Spearman's rank correlation. A significant correlation between a decrease in expression and increasing methylation density ($rho=0.77$, $p<.001$, $df=19$) was observed.

Odds ratios were also calculated for each region of interest to assess the strength of the inverse association between *RUNDC3B* expression and the presence of methylation. Regions 2,

3, 4, 5 and 6 showed a significant inverse association between CGI methylation and *RUNDC3B* expression: Region 1) OR: 6.75, 95% CI: 0.93-49.23, p=.06; Region 2) OR: 84, 95% CI: 4.51-1564.34, p=.003; Region 3) OR: 135, 95% CI: 4.87-3744.64, p=.004; Region 4) OR: 78.2, 95% CI: 3.31-1849.13, p=.007; Region 5) OR: 38.5, 95% CI: 2.92-508.49, p=.006; Region 6) OR: 141.67, 95% CI: 5.14-3907.44, p=.004. In the lymphoid malignancies, regions 2, 3, 4 and 6 were methylated in each cell line that did not express *RUNDC3B* and were not methylated in the cell lines that did express *RUNDC3B*. The relationship between methylation and gene expression in the solid tumors was less pronounced suggesting that different regulatory mechanisms may be accountable in these tumors.

The *RUNDC3B* CGI lies within an intron of ATP-binding cassette sub-family B member 1 (*ABCB1*) which encodes a P-glycoprotein that is responsible for transporting molecules, including therapeutic drugs, across cellular membranes [7]. Methylation of the *ABCB1* promoter has been shown to contribute to progression in prostate cancer and acute myeloid leukemia [8,9]. To determine if methylation of the *RUNDC3B* promoter also affected regulation of *ABCB1*, quantitative PCR for *ABCB1* was also performed. Expression of *ABCB1* was consistent across samples regardless of methylation status.

Methylation and expression trends in cell lines are representative of patient samples

To determine if the methylation and expression patterns present in cell lines also hold true in patient samples, the methylation and expression present in ALL, AML, CLL, and DLBCL patients were explored. Methylation profiles generated in our laboratory by enriching for

methylated DNA using the Methylated CpG Island Recovery Assay (MIRA) followed by next-generation sequencing (unpublished data) in 20 ALL patients and healthy cord blood revealed a peak that spans the 6 amplicons within the *RUNDC3B* CGI, chr7:87256845-87258468 (**Figure 3**). This peak was present in 17 of 20 ALL patients and in only 1 of 10 healthy cord blood samples ($p=1.34x10^{-4}$, Fisher's exact test). RNA-seq data for the same 20 patients revealed an average FPKM (fragments per kilobase of exon per million fragments mapped) for the group of 0.22 (range 0 – 1.19) indicating that there is virtually no expression of *RUNDC3B* in these samples. Methylation profiles have also been generated for 11 CLL patients using reduced representation bisulfite sequencing (RRBS) [10]. The methylation values were low across CLL patients with an average methylation score of 0.096 (**Figure 3**, **Table 3**). In some cases, high methylation values were observed at a particular CpG site; however, the average methylation level remained low across the region. No expression data was available for these patients; therefore, to determine the expression of *RUNDC3B* in CLL patient samples, a publically available data set comprising 68 CLL patients (GSE10138) was utilized [11]. The average expression value across all patients fell within the second quartile confirming that RUNDC3B is expressed in these patients (**Figure 4A**). Two additional lymphoma data sets were analyzed from the Cancer Genome Atlas (TCGA) using the UCSC Cancer Genomics Browser representing AML patients (194 samples; LAML DNA methylation data; LAML gene expression pancan normalized) and DLBCL patients (48 samples; DLBC DNA methylation data; DLBC gene expression pancan normalized). The methylation and expression profiles were consistent with

data from the AML and DLBCL cell lines and showed lower levels of DNA methylation and higher levels of expression in AML patients when compared to DLBCL patients (**Figure 4B, C**). Although this does not represent all of the diseases included in our study, in the cases of ALL, AML, CLL, and DLBCL the patient data is consistent with our findings in cell lines.

The MAPK pathway is dysregulated in the Nalm 6 cell line

It is hypothesized that RUNDC3B is an effector protein of the Rap2 GTPase and activation of Rap2 has been shown to regulate the MAPK pathway. In addition to a RUN domain, 6 MAPK D docking domains were identified in the RUNDC3B protein sequence suggesting a potential role for RUNDC3B as a mediator between MAPK genes and Rap2. MAPK signaling pathway PCR arrays were utilized to determine whether key genes were up- or down-regulated in the Nalm 6 cell line which was methylated in each region of the RUNDC3B promoter. A total of 23 genes were upregulated and 6 genes were downregulated in the Nalm 6 cell line including genes with MAPK-induced expression and transcription factors with MAPK dependent activation (**Table 4**).

Discussion

The human *RUNDC3B* CGI is 1486 base pairs, contains 132 CpG sites and harbors 2 conserved transcription factor binding sites (TFBS), early growth response-3 (EGR-3) and activating protein-2 (AP-2). Interestingly, EGR3- is a zinc finger protein implicated in neuronal, muscle, and lymphocyte development [12]. The EGFR-3 TFBS also lies within a region of DNase hypersensitivity which is associated with active transcription. A survey of publically

available DNA methylation data and DNase hypersensitivity data revealed a 1:1 correlation between the absence of methylation and the presence of a DNase hypersensitivity site and vice versa in the *RUNDC3B* CGI [13]. It is likely that the direct methylation of the EGR-3 TFBS interferes with the *trans*-acting regulatory interaction between EGR-3 and the *RUNDC3B* promoter.

Considering that RUNDC3B is a putative Rap-2 binding protein, and because it contains characteristic structural MAPK binding domains, we hypothesize that it is an effector of the MAPK signaling cascade (**Figure 5**). Rap2A interacts directly with upstream MAPK signaling element MAP4K4 and thus increased Rap2A activity can perpetuate downstream signaling [14]. If not properly regulated, Rap2B activity can increase phospholipase C, epsilon 1 (PLCE1) activity which can lead to the activation of Ras signaling which may lead to increased cell growth and differentiation, and ultimately, tumorigenesis [15]. Downregulation of c-Jun and c-Fos—downstream effectors of Rap2 proteins, was observed in Nalm 6. Together, Jun and Fos combine to form the AP-1 transcription factor which is activated by the JNK pathway to regulate transcriptional activation of genes. Loss of AP-1 expression results in deregulated transcription of genes necessary for differentiation and proliferation. As a Rap2-interacting protein, RUNDC3B may play a role in the activation of c-Jun and c-Fos and the loss of RUNDC3B may lead to the down regulation of these genes.

An alternative function for RUNDC3B may also be inferred based on recent reported interactions between RUNDC3B and casein kinase 1 gamma 1 and 2 (CSNK1G1/2) [16]. Both

CSNK1G1 and CSNK1G2 are serine and threonine kinases involved in canonical Wnt signaling. A clear role has been established between abnormal Wnt signaling and the development of lymphoid cancers [17, 18]. Specifically, the casein kinases are responsible for phosphorylating the transmembrane proteins Lrp5 and Lrp6 [19]. This enables the formation of the signalosome that perpetuates Wnt signaling and β-catenin to transcribe Wnt genes. Therefore, the absence of *RUNDC3B* expression may alter the ability of CSNKIG1/2 to contribute to the formation of the signalosome resulting in the aberrant regulation of Wnt signaling.

In summary, aberrant DNA methylation of the RUNDC3B CGI results in the repression of the gene. Methylation was observed in several solid tumor cell lines, and in samples representing lymphoid malignancies with higher methylation densities being observed in lymphoid samples that are derived from the bone marrow and the germinal center. Other lymphoid malignancies such as CLL and MCL expressed *RUNDC3B* and were not methylated. Therefore, RUNDC3B methylation may prove to be a useful biomarker for diagnosis, prognosis and in tracking minimal residual disease in malignancies of the bone marrow and germinal center which include ALL, BL, FL and DLBCL.

Conflict of interest

The authors have no potential conflicts to disclose.

Acknowledgements

This work was supported by the National Institutes of Health NCI R00 CA132784 (K.H. Taylor). We kindly thank Darren Hawkins, Emily Shank and Md Almamun for generating the figures included in this manuscript.

References

1. Robertson KD, Wolffe AP. DNA methylation in health and disease. *Nat Rev Genet* 2000; **1**:11-19.

2. Taylor KH, Pena-Hernandez KE, Davis JW, Arthur GL, Duff DJ, Shi H, *et al*. Large-scale CpG methylation analysis identifies novel candidate genes and reveals methylation hotspots in acute lymphoblastic leukemia. *Cancer Res* 2007; **67**:2617-2625.

3. Wang MX, Wang HY, Zhao X, Srilaha N, Zheng D, Shi H, *et al*. Molecular detection of B-cell neoplasms by specific DNA methylation biomarkers. *Int J Clin Exp Pathol* 2010; **3**:265-279.

4. Raguz S, De Bella MT, Slade MJ, Higgins CF, Coombes RC, Yague E. Expression of RPIP9 (Rap2 interacting protein 9) is activated in breast carcinoma and correlates with a poor prognosis. *Int J Cancer* 2005; **117**:934-941.

5. Rountree MR, Bachman KE, Herman JG, Baylin SB. DNA methylation, chromatin inheritance, and cancer. *Oncogene* 2001; **20**:3156-3165.

6. Walter, SD. Point estimation of the odds ratio in sparse 2 × 2 contingency tables In *Biostatistics*, MacNeill IB, Umphrey GJ, Reidel D (eds). Springer: Netherlands, 1987; 71-102.

7. Fardel O, Lecureur V, Guillouzo A. The P-glycoprotein multidrug transporter. *Gen Pharmacol* 1996; **27**:1283-1291.

8. Enokida H, Shiina H, Igawa M, Ogishima T, Bassett WW, Anast JW, *et al*. CpG hypermethylation of *MDR1* gene contributes to the pathogenesis and progression of human prostate cancer. *Cancer Res* 2004; **64**:5956-5962.

9. Toyota M, Kopecky KJ, Toyota MO, Jair KW, Willman CL, Issa JP. Methylation profiling in acute myeloid leukemia. *Blood* 2001; **97**:2823-2829.

10. Pei L, Choi JH, Liu J, McCarthy B, Wilson JM, Speir E, *et al*. Genome-wide DNA methylation analysis reveals novel epigenetic changes in chronic lymphocytic leukemia. *Epigenetics* 2012; **7**(6):567-78.

11. Friedman DR, Weinberg JB, Barry WT, Goodman BK, Volkheimer AD, Bond KM, *et al*. A genomic approach to improve prognosis and predict therapeutic response in chronic lymphocytic leukemia. *Clin Cancer Res* 2009; **15**(22):6947-55.

12. Patwardhan S, Gashler A, Siegel MG, Chang LC, Joseph LJ, Shows TB, *et al*. EGR3, a novel member of the Egr family of genes encoding immediate-early transcription factors. *Oncogene* 1991; **6**:917-928.

13. ENCODE Project Consortium. An integrated encyclopedia of DNA elements in the human genome. *Nature* 2012; **489**:57-74.

14. Machida N, Umikawa M, Takei K, Sakima N, Myagmar BE, Taira K, *et al*. Mitogen-activated protein kinase kinase kinase kinase 4 as a putative effector of Rap2 to activate the c-Jun N-terminal kinase. *J Biol Chem* 2004; **279**:15711-15714.

15. Evellin S, Nolte J, Tysack K, vom Dorp F, Thiel M, Weernink PA, Jakobs KH, *et al*. Stimulation of phospholipase C-epsilon by the M3 muscarinic acetylcholine receptor mediated by cyclic AMP and the GTPase Rap2B. *J Biol Chem* 2002; **277**:16805-16813.

16. Vinayagam A, Stelzl U, Foulle R, Plassmann S, Zenkner M, Timm J, *et al*. A directed protein interaction network for investigating intracellular signal transduction. *Sci Signal* 2011; **4**:rs8.

17. Khan NI, Bradstock KF, Bendall LJ. Activation of Wnt/beta-catenin pathway mediates growth and survival in B-cell progenitor acute lymphoblastic leukaemia. *Br J Haematol* 2007; **138**:338-348.

18. Reya T, Duncan AW, Ailles L, Domen J, Scherer DC, Willert K, *et al*. A role for Wnt signalling in self-renewal of haematopoietic stem cells. *Nature* 2003; **423**:409-414.

19. Bilic J, Huang YL, Davidson G, Zimmermann T, Cruciat CM, Bienz M, *et al*. Wnt Induces LRP6 Signalosomes and Promotes Dishevelled-Dependent LRP6 Phosphorylation. *Science* 2007; **316**:1619-1622.

Figure Legends

Figure 1. *RUNDC3B* promoter and amplicons. The *RUNDC3B* promoter is present within an intron of the *ABCB1* gene and contains an annotated CGI (green bar). The methylation status of regions 1-6 was determined. A conserved EGR-3 transcription factor binding site is present within region 3 and a conserved AP2 transcription factor binding site is located within region 4. Each of these transcription factor binding sites is located within a region of DNaseI hypersensitivity further supporting the regulatory potential of this region.

Figure 2. *RUNDC3B* methylation and expression in cell lines and controls. The methylation status of regions 1-6 was determined. Samples are organized based on tissue type, L=lymphoid, M=myeloid, S=solid tumor, C=control tissue. Methylation density (MD) was determined for the entire region and given a numeric value. The expression status for each sample was also determined, Y=C_T<35, N=C_T≥35.

Figure 3. *RUNDC3B* methylation in ALL and CLL patients. *RUNDC3B* associated methylation data was extracted from previously generated ALL (unpublished data) and CLL [10] methylation profiles. RRBS data is shown for each CLL patient. Green and red bars represent unmethylated and methylated CpG sites respectively. MIRA-seq data was utilized for peak identification in ALL patient samples. The location of a peak spanning the *RUNDC3B* CGI and present in 17 out of 20 ALL samples is shown.

Figure 4. Methylation and expression of RUNDC3B in patient samples. The results shown here are based upon data generated by the TCGA Research Network: http://cancergenome.nih.gov/. **A.** Expression of *RUNDC3B* in 41 CLL patients and 11 normal controls. The red bars and the left axis represent normalized counts. The blue squares and the right axis represent the percentile rank within the sample. **B.** Methylation and expression in AML patients. Methylation shown in gray box (left panel) for 11 cytosines (vertical bars) present in the RUNDC3B CGI. Proportional expression is shown in right panel. **C.** Methylation and expression in DLBCL patients. Proportional methylation shown in gray box (left panel) for 11 cytosines (vertical bars) present in the RUNDC3B CGI. Proportional expression is shown in right panel.

Blue to red scale represents lowest to highest methylation and expression values.

Figure 5. Proposed role of RUNDC3B in the MAPK signaling pathway. RUNDC3B is hypothesized to interact with Rap2 based on homology with RUNDC3A. In this model, Rap2 activates RUNDC3B which then interacts with MAP kinases to influence downstream responses.

Table 1. Description of cell lines and healthy samples. Samples are grouped by tissue type. L=lymphoid, M=myeloid, S=solid tumor, C=healthy controls

Table 2. RUNDC3B primer sequences and amplicon characteristics. *The restriction enzyme BstUI was used in all COBRA reactions. COBRA reactions were performed for regions 1, 2, 5, and 6. MSP reactions were performed for regions 3 and 4.

Table 3. RRBS data for RUNDC3B in CLL patients [10]. For each patient, the number of CpG sites analyzed is provided. The average and median are in reference to the total number of CpG sites within the RUNDC3B CGI. Low and high represent the range of values across all CpG sites.

Table 4. Differential expression of MAPK pathway genes in a RUNDC3B methylated leukemia cell line versus a RUNDC3B unmethylated control bone marrow sample.

Table 1. Description of cell lines and healthy control samples.

	Sample	Description
L	MHH Call 3	B-Acute lymphoblastic leukemia cell line
	Nalm 6	B-Acute lymphoblastic leukemia cell line
	Jurkat	T-Acute lymphoblastic leukemia cell line
	Mec-1	Chronic lymphocytic leukemia cell line
	DB	Diffuse large B-cell lymphoma cell line
	Granta-519	Mantle cell lymphoma cell line
	RL	Follicular lymphoma cell line
	Raji	Burkitt's cell line
	Daudi	Burkitt's cell line
M	U226B1	Multiple myeloma cell line
	KG-1	Acute myeloid leukemia cell line
S	MDA MB 231	Breast carcinoma cell line
	Hela	Cervical carcinoma cell line
	A431	Epidermal carcinoma cell line
	A549	Lung carcinoma cell line
	WiDr	Colorectal adenocarcinoma cell line
C	GM06990	Lymphoblast cell line
	GM00536	Fibroblast cell line
	BM	Bone marrow B cells
	CB	Cord blood B cells

Samples are grouped by tissue type. L=lymphoid, M=myeloid, S=solid tumor, C=healthy controls

Table 2. RUNDC3B primer sequences and amplicon characteristics.

Primer	Forward Sequence/Reverse Sequence	Amplicon Size	COBRA Digest Sizes*
Region 1	5'-GTTTTAGGATTTTGAGGGAGTAGTTTAG-3' 5'-CCCAAAAACTAATAAACAACAACAC-3'	301 bp	125, 107 and 69 bp
Region 2	5'-TTGTTGTTTATTAGTTTTTGGGAGG-3' 5'-CCCCTTACCTATAACCAAACTTTAAC-3'	176 bp	93 and 83 bp
Region 3 Methylated	5'-GTGGTTATTGGCGGTAGTTAGC-3' 5'-GCGAACCTTTTAAAACAACGA-3'	104 bp	MSP
Region 3 Unmethylated	5'-GTGTGGTTATTGGTGGTAGTTAGTG-3' 5'-CACAAACCTTTTAAAACAACAAA-3'	107 bp	MSP
Region 4 Methylated	5'-GGGTTTTGTCGTTGTTTTTC-3' 5'-CTTAAAAAAATTCTCGCTCGA-3'	374 bp	MSP
Region 4 Unmethylated	5'-GGGTTTTGTTGTTGTTTTTT-3' 5'-CCTACTTAAAAAAATTCTCACTCAA-3'	378 bp	MSP
Region 5	5'-GAGAATTTTTTTAAGTAGGTGTGG-3'	249 bp	143 and 106 bp

*The restriction enzyme BstUI was used in all COBRA reactions. COBRA reactions were performed for regions 1, 2, 5, and 6. MSP reactions were performed for regions 3 and 4.

	5’-AAAACCCAAAACTCTCAACCC-3’		
Region 6	5’-GTGGAGAGGAGGAATTTGATTAT-3’ 5’-AAACTAACACAAAATCCAAAACTAC-3’	236 bp	93, 80, and 63 bp

Table 3. RRBS data for RUNDC3B in CLL patients [10].

Patient ID	CpG sites	Average	Median	Low	High
CLL_1	61	0.13	0.04	0	0.96
CLL_2	55	0.09	0.02	0	0.54
CLL_3	52	0.12	0.04	0	0.73
CLL_4	60	0.06	0.02	0	0.52
CLL_5	52	0.11	0.03	0	0.68
CLL_6	51	0.10	0.03	0	0.50
CLL_7	54	0.08	0	0	0.58
CLL_8	66	0.10	0.02	0	0.65
CLL_9	51	0.07	0	0	0.48
CLL_10	51	0.08	0	0	0.56
CLL_11	51	0.12	0.08	0	0.44

For each patient, the number of CpG sites analyzed is provided. The average and median are in reference to the total number of CpG sites within the RUNDC3B CGI. Low and high represent the range of values across all CpG sites.

Table 4. Differential expression of MAPK pathway genes in a RUNDC3B methylated leukemia cell line versus a RUNDC3B unmethylated control bone marrow sample.

Upregulated Genes		Down Regulated Genes	
Symbol	**Fold Change**	**Symbol**	**Fold Change**
CCND3	37.79	BRAF	-5.5
CDC42	8.82	CCNA1	-71.51
CDK6	46.53	CCND2	-82.14
CDKN1A	23.26	FOS	-17.88
CDKN2C	10.13	HSPA5	-8.94
CREB1	13.36	JUN	-44.12
ETS1	4.72		
ETS2	10.85		
GRB2	18.89		
HRAS	10.13		
HSPB1	93.05		
KRAS	10.85		
MAP2K3	6.68		
MAP3K1	5.06		
MAP4K1	7.16		
MAPK13	8.82		
MAPK6	9.45		
MAPKAPK2	13.36		
MAPKAPK3	4.41		
MAX	10.85		
NRAS	7.67		
RB1	37.79		
SMAD4	7.67		

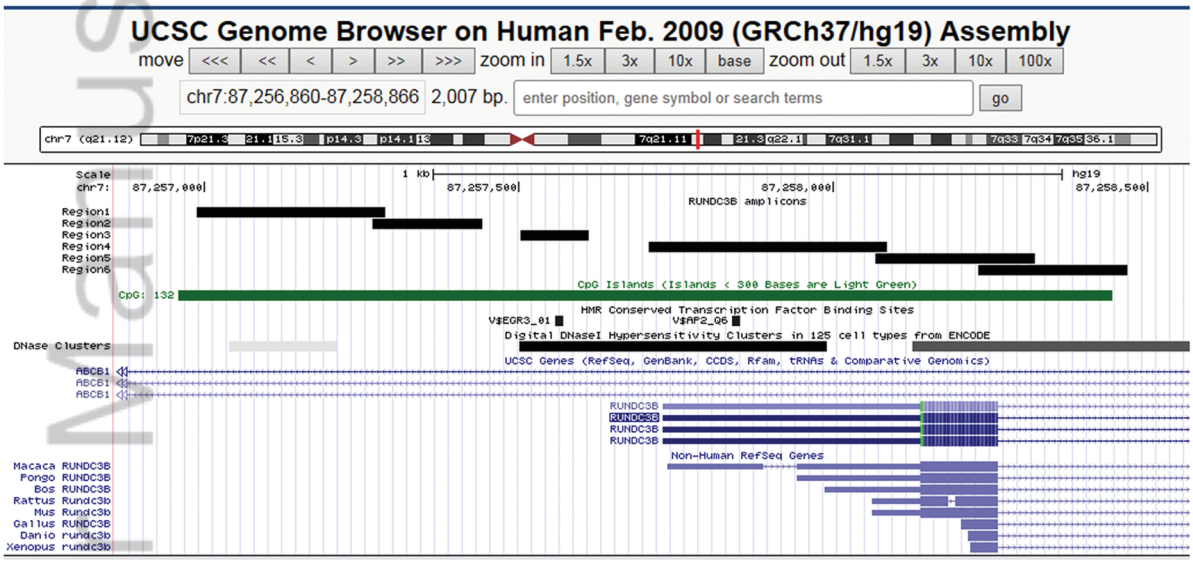

HON_2238_F1.tif

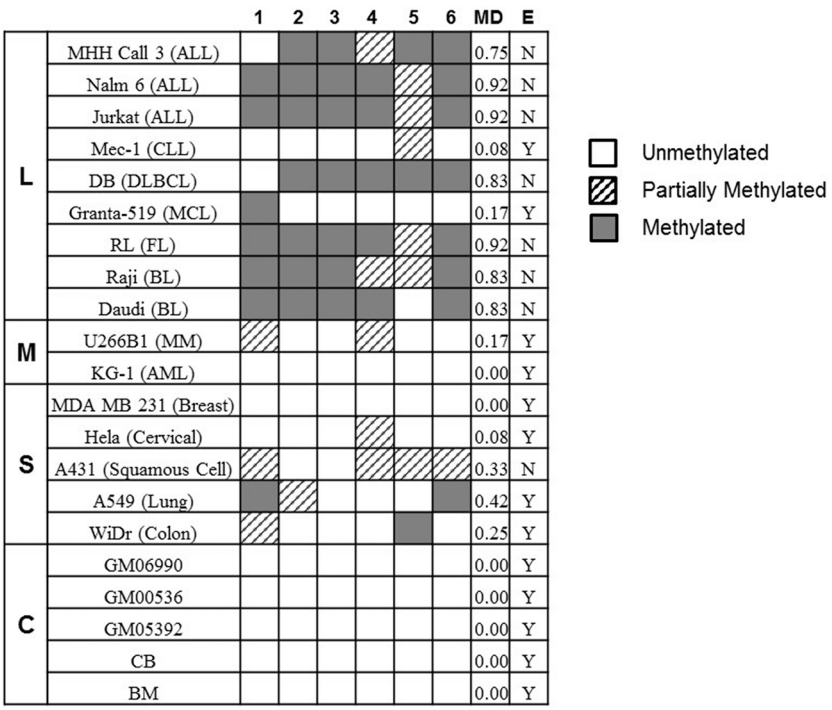

HON_2238_F2.tif

HON_2238_F3.tif

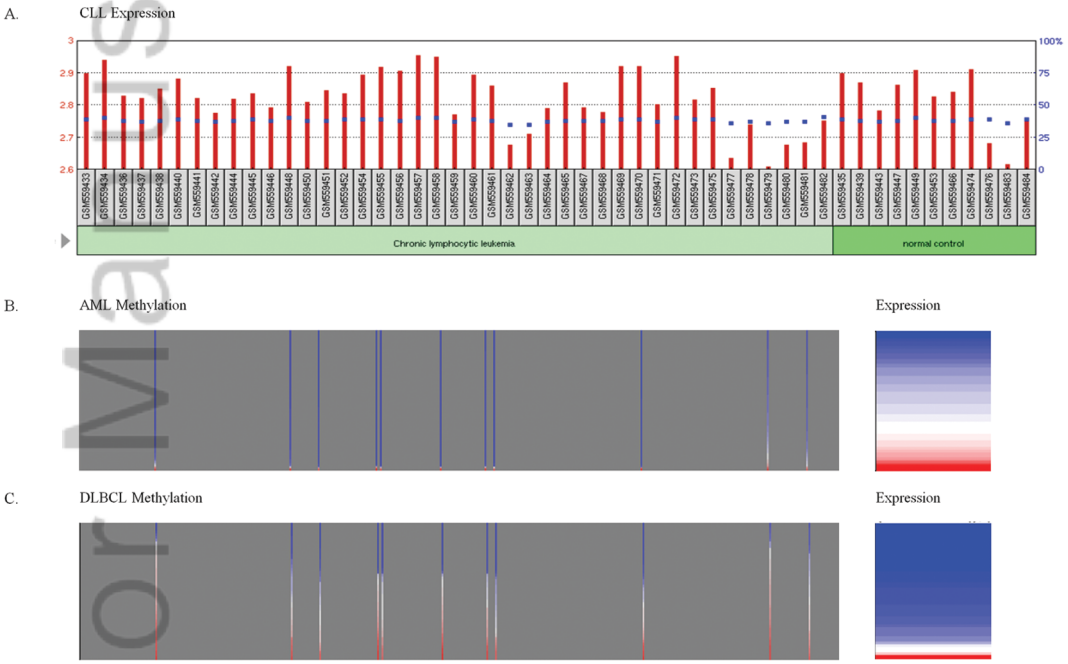

HON_2238_F4.tif

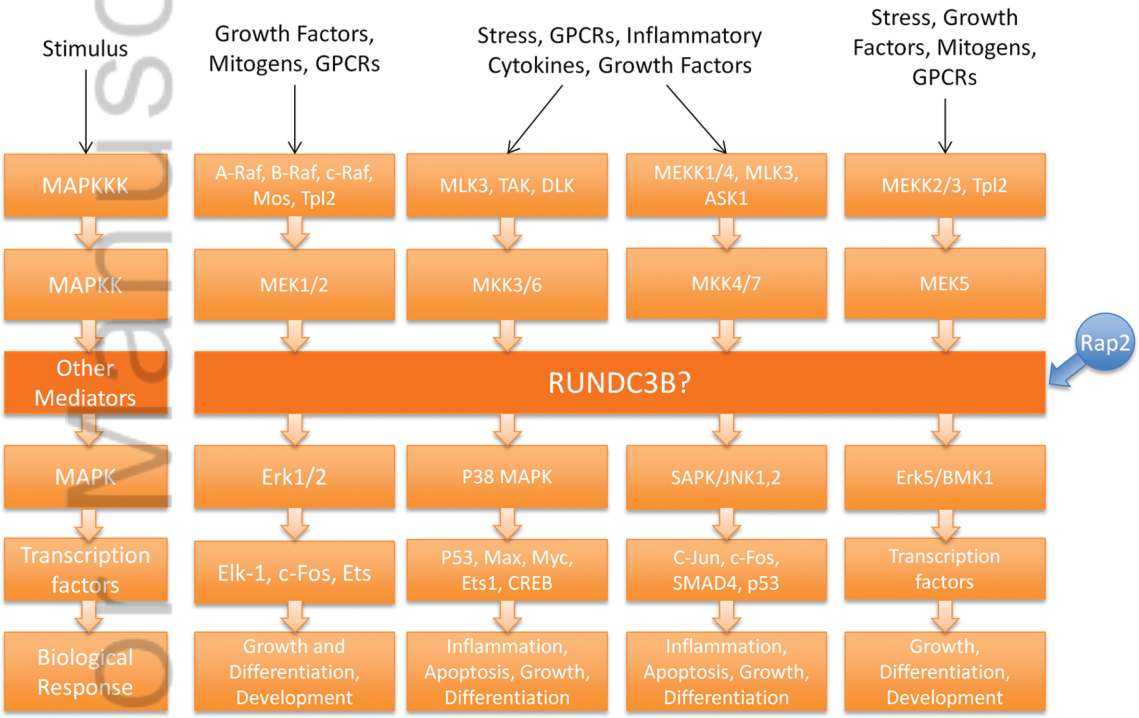

HON_2238_F5.tif